Advances in Material Research, *Vol. 3, No. 1 (2014) 259-269*
DOI: http://dx.doi.org/10.12989/amr.2014.3.1.259

Preparation and characterization of boron-nitrogen coordination phenol resin/SiO_2 nanocomposites

J.G. Gao*, D. Zhai and W.H. Wu

College of Chemistry & Environment Science, Hebei University, Baoding 071002, P. R. China

(Received May 216, 2013, Revised September 23, 2013, Accepted September 24, 2013)

Abstract. The boron-nitrogen-containing phenol-formaldehyde resin (BNPFR)/SiO_2 nanocomposites (BNPFR/SiO_2) were synthesized in-situ, and structure of BNPFR/SiO_2 nanocomposites was characterized by FTIR, XRD and TEM. The loss modulus peak temperature T_p of BNPFR/SiO_2 nanocomposites cured with different nano-SiO_2 content are determined by torsional braid analysis (TBA). The thermal degradation kinetics was investigated by thermogravimetric analysis (TGA). The results show that nano-SiO_2 particulate with about 50 nm diameter has a more uniformly distribution in the samples. The loss modulus peak temperature T_p of BNPFR/SiO_2 nanocomposite is 214 ^oC when nano-SiO_2 content is 6 wt%. The start thermal degradation temperature T_{di} is higher about 30 ^oC than pure BNPFR. The residual rate (%) of nanocomposites at 800 ^oC is above 40 % when nano-SiO_2 content is 9 %. The thermal degradation process is multistage decomposition and following first order.

Keywords: boron-nitrogen-coordination; phenol-formaldehyde resin; nanocomposites; nano-SiO2; thermal analysis

1. Introduction

Phenolic-formaldehyde resin (PFR) is an excellent thermosetting resin, which has the good mechanical properties and heat resistance. They are widely used to prepare fiberglass-reinforced laminate, molding compounds, thermal insulation materials, coating, and adhesive, especially in the high-technique fields, such as spaceflight, rocketry, and so on (De *et al*. 2007). However, the phenolic hydroxyl, ether bond and methylene in the structure of phenolic resin are easily oxidized. These shortcomings will decrease the heat resistance, oxidation resistance and mechanical properties of materials. In order to improve its performance, the phenolic resins called boron-containing phenol-formaldehyde resin (BPFR) were obtained by introducing inorganic element boron into the resolve and novolac phenolic resin (Abdalla *et al*. 2003, Martin *et al*. 2006, Liu *et al*. 2002, Gao *et al*. 2004 and 2010). The effectiveness of the borate as the flame-retardants in various materials has been explained by their formation of non-penetrable glass coating in these materials when they are heated. The glass coatings exclude oxygen and prevent further propagation combustion. However, the general BPFR is extremely sensitive to moisture or water, because of the unsaturating property of boron atom. These shortcomings will restrict the range of

*Corresponding Author, Professor., E-mail: gaojg@mail.hbu.edu.cn

http://www.techno-press.org/?journal=amr&subpage=7 ISSN: 2234-0912 (Print), 2234-179X (Online)

applications and storage condition of BPFR. In order to improve the hydrolytic stability and physical properties of BPFR, many researchers have done some works, such as modified by B-N or, B-O coordination, layered-silicate nanoparticles, nanoparticles, etc (Gao *et al*. 2004 and 2010, Wang *et al* 2008, Hoofel *et al*. 1975). But the coordination structure of boron atom in foregoing reported resins has not fully formed in the synthesized process, so they have yet not very good water resistance.

Organic/inorganic hybrid nanocomposites prepared in situ created inorganic phase method have become a fascinating new field of research in materials science (Siramanont *et al*. 2009, Yuvaraj *et al*. 2010). Nanostructure hybrid organic-inorganic composites typically exhibit superior mechanical properties than the parent materials. Many polymers, including polyimide, epoxy resin, polystyrene, poly (dimethyl siloxane) *et al*, have been used to produce hybrid nanocomposites (Rund, *et al*. 2012, Nayak *et al*. 2012, Kusmono *et al*. 2010). Chiang C. and Byun H.Y. *et al* had reported that the common phenol-formaldehyde resins were modified by nanosilica formed from hydrolytic condensation of tetraethoxysilane or organic-montmorillonite (Chiang *et al*. 20004, Byun *et al*. 2001).

We have reported the synthesis of organic-inorganic hybrid boron-containing phenol-formaldehyde resin/SiO_2 nanocomposites, but it is not contained boron-nitrogen coordination structure (Gao *et al*. 2008). Wang D. C. *et al* had reported the preparation and thermal stability of general boron-containing phenolic resin/clay nanocomposites (Wang *et al*. 2008). But these resins have yet not good water resistance. To the best of our knowledge, there is no precedent report on the synthesis of boron-nitrogen coordination containing phenol-formaldehyde resin (BNFR)/ SiO_2 nanocomposites from Phenol, boric acid, aminoethyl alcohol and paraformaldehyde, and in situ created nano-SiO_2. In this work, the boron-nitrogen coordination containing phenol-formaldehyde resin/SiO_2 nanocomposite (BNFR/SiO_2) was systhesized. The structure and the distributions of silicon element were characterized by Fourier-transform infrared spectroscopy (FTIR), energy dispersive X-ray spectrometry (EDS) and transmission electron microscope (TEM), respectively. The loss modulus peak temperature T_p was determined by torsional braid analysis (TBA). The kinetics of thermal degradation and thermal stability were determined by thermograavimetry analysis (TGA).

2. Experimental details

2.1 Materials

Phenol, boric acid, aminoethyl alcohol, paraformaldehyde, sodium hydroxide, ethanol, 37% aqueous formalin and acetone were all analytically pure grade, which were supplied by Tianjin Chemical Co. China; Tetramethoxysilane (TMOS) was supplied by Jintan Chemical Co. of Zhejiang, China.

2.2 Synthesis of BNFR/SiO2 nanocomposites

The aminoethylbiphenli borate was synthesized according to the method from literature (Zhai *et al*. 2008). 0.2 mol Phenol, 0.1 mol boric acid and 30 mL toluene were put into a four-necked round bottom flask, equipped with a stirrer, a thermometer and an oil-water segregator. The mixture was heated to 120 ^oC and held at this temperature for 30 min, then was gradually heated to 180^oC and

maintained at this temperature for 3 h until theoretic quality water was removed out from reaction system and the biphenol borate was obtained. Then the system temperature was reduced to 60°C and added 0.1 mol aminoethyl alcohol to it, and reaction continuous for another 4 h. The water formed in the reaction and un-reactants were removed in vacuum. The product was wished with water and extracted with ethyl ether, then dried with anhydrous $MgSO_4$. The aminoethylbiphenli borate (AEBPB) was obtained after removed ethyl ether in vacuum, which structure as Scheme 1.

First, 1 mol AEBPB, 2.6 mol paraformaldehyde, 1 g oxalic acid and 30 moL toluene were put into a four-necked round bottom flask, equipped as forenamed. The mixture was heated to 120°C and held at this temperature for 2 h. The toluene and water formed in the reaction were removed in vacuum. In the second step, 80 mL ethanol was added into this system with 7.15 g TMOS (3 wt% SiO_2) dropping at 80°C, and continued reaction for another 3 h. Finally, the BNPFR/SiO_2 nanocomposites as a semi-transparent yellow solid was obtained after the water and ethanol were removed in vacuum.

By changing the dosage of TMOS, the BNPFR/SiO_2 nanocomposites with different SiO_2 content were obtained.

The general boron-containing phenol-formaldehyde resin (BPFR) was synthesized according to the method from literature (Liu *et al*. 2002), the mole ratio of phenol : formaldehyde : H_3BO_3 is 3 : 3.9:1.

2.3 Equipment and Characterization Procedures

FTIR spectrometer (FTS-40, Bro-Rad, USA) was used to investigate the structure of BNPFR/SiO_2 nanocomposite. The resin was dissolved in acetone and then coated as a thin film on a potassium bromide plate. When the solvent in the film was completely evaporated in vacuum, the potassium bromide plate was scanned from 400 cm^{-1} to 4000 cm^{-1} by the FTIR spectrometer.

The distribution of silica was characterized by means of energy dispersive X-ray spectrometry (EDS). Resin was heated and pressed to 1.0 mm thickness plate, and then was determined by EDS (Thermo Noran Co. USA), the accelerate voltage was 25 kV and resolution was 128×128.

A transmission electron microscope (TEM, JEM-100CX, JEOL, Japan) was used to determine the size and distribution of nanosilica. The sample was prepared by frozen sectioning method. The testing voltage was 100 KV and resolution was 0.14 nm.

The thermal stability of the samples was characterized by using a thermogravimetric analyzer (TGA, Pyris-6, Perkin-Elmer, US) operating under a nitrogen atmosphere. About 10 mg BNPFR/SiO_2 power cured at 180°C for 2h was introduced into the thermobalance, and then heated from 25°C to 800°C at 20°C/min heating rate and in nitrogen flow 20 mL/min.

A cleaned glass fiber braid was first dipped in resin-acetone solution for about 30 min, and then the acetone was completely evaporated in vacuum. The specimens were cured at 185℃ in an oven for 2 h. Then, they were removed and cooled to room temperature, and the dynamic mechanical properties of BNPFR/SiO_2 nanocomposites were investigated with a torsional braid analyzer (TBA, GDP-4, Jilin University, China) at the heating rate of 2℃ min^{-1}.The maximal mechanical loss peak temperature (T_p) could be obtained. Because it has one-to-one relationship between T_g and mechanical loss peak temperature T_p, these T_g temperatures were obtained by adopting the above method.

The hydrolytic stability of resins was determined by a half-life of acid-base titration method (Shen *et al*. 1999). The 0.1 mol/L NaOH solution in which the NaOH mol amount equivalent to half the mol amount of boron in resin was added into mixed solution of 50 mL water and 5 mL

glycerol (containing 4 drop phenolphthalein) with agitated, and recording the time of changed color.

3. Results and discussion

3.1 Structure of BNPFR/SiO_2 nanocomposite

Fig. 1 is the FTIR spectra of BNPFR and BPFR. According to data from literature (Shen *et al*. 1999, Shen 1982, Gao 1990), the principal absorption bands of BPFR are: the hydroxyl group –OH at 3300-3500 cm^{-1}, the benzene ring at 1600 cm^{-1} and 750 cm^{-1}, the phenol borate B-O at 1350 cm^{-1}, the methylene group -CH_2- at 1450 cm^{-1} and 2920 cm^{-1}, benzyl hydroxyl group at 1250 cm^{-1}, ether linkage C-O at 1100 cm^{-1}, C-N at 1580 cm^{-1}, -OH and –NH at 3300-3500cm^{-1}. Comparison the FTIR spectra of BNPFR and BPFR in Fig. 1, it is seen that the absorption band of B-O bond at 1350~1380 cm^{-1} in BNPFR has disappeared, which shows that the coordination structure of B-N had formed in BNPFR. The result is coincident with that the result of IR absorption band of borate will disappear in B-O coordination structure (Tu *et al*. 1981, Hoofel *et al*. 1975. Gao *et al*. 1990). Another, it can also see that the absorption band of hydroxyl group –OH at 3300-3500 cm^{-1} in the BNPFR has disappeared, which shows that the aminoethylbiphenli borate has formed.

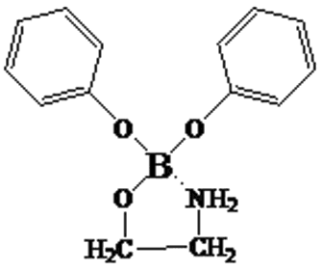

Schem. 1 molecular structure of aminoethylbiphenli borate

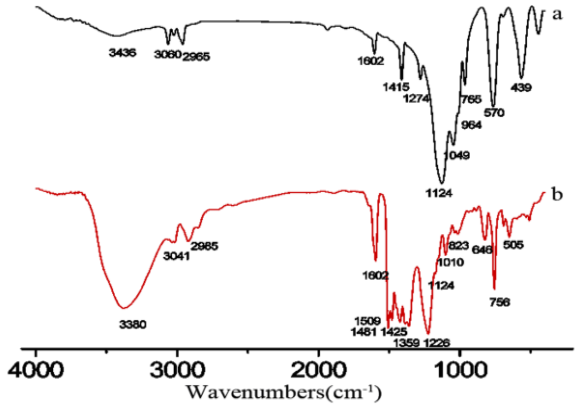

Fig. 1 FTIR spectra of BNPFR and BPFR

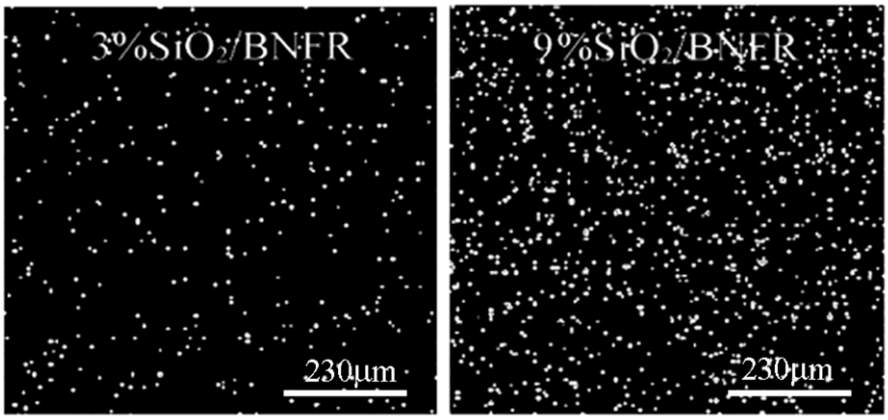

Fig. 2 The silicon element distributions of 3 and 9 wt% /BNCFR/SiO_2

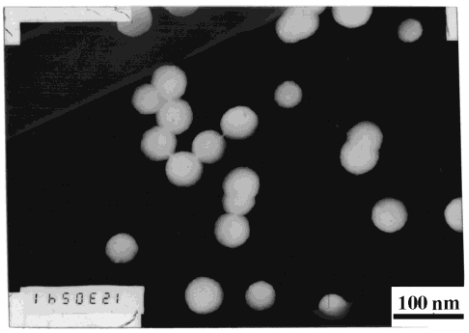

Fig. 3 TEM images of 9%SiO_2/BNCFR nanocomposites

3.2 EDS and TEM analysis

Fig. 2 shows the silicon element distribution in the 3, 9 wt% BNPFR/SiO_2 nanocomposites, respectively. In the Fig. 2, the white point is SiO_2 particulate which was formed from TMOS. Comparison the silicon element distribution in Fig. 2, it can find out that the silicon element has a more uniformly distributed, only a small amount of conglomeration, and the density of SiO_2 particulate increase with the increasing additive amount of TMOS.

Dispersion and size of nano-SiO_2 is observed with TEM and shown in Fig. 3. As seen from Fig. 3, the size of nano SiO_2 is about 40-60 nm in diameter and more uniformly dispersed in the BNPFR matrix. The results of EDS and TEM analysis show that in-situ formed nano-SiO_2 from TMOS had more homogeneous distributed in the BNPFR and organic-inorganic hybrid nanocomposite had been obtained.

3.3 Torsional braid analysis

Because the glass transition temperature (T_g) can be used effectively to monitor the molecular motion and curing reaction, and has a relationship between the T_g and the degree of cure. T_g has

been used directly as a parameter of heat-resistance for polymer and as a parameter for conversion in the analysis of reaction kinetic models for thermosetting polymers (Gillham 1997). TBA method can be used to determine the T_g of the thermosetting system, and It is particularly useful at high conversion and after vitrification because of the non-linearity of T_g versus conversion (Venditti *et al*. 1997). DSC is usually used to determine the T_g of polymer, but it is not a best method for thermosetting polymers, especially at higher conversion, because the shift of DSC curve will be very small and inconspicuous at that time. TBA is usually used to determine the maximal mechanical loss temperature (T_p) of thermosetting polymers (Gillham 1997, Brandalise *et al*. 2009, Doyle *et al*. 2003), which has a one-to-one relationship between T_g and T_p. The higher T_p, the higher T_g is, which depends on the curing conditions, such as amount of cross-linked agent, cure temperature and time.

Fig. 4 is the TBA curves of BNPFR/SiO_2 nanocomposites curing 120 min at 180°C. As seen from Fig. 4, the loss modulus curve has one biger and relatively narrow peak at 200°C for 3 wt% SiO_2 BNPFR/SiO_2 nanocomposite, the 6 wt% SiO_2 BNPFR/SiO_2 nanocomposite has a relatively broad peak at 214°C, which is 14°C higher than that of 3 wt% SiO_2 BNPFR/SiO_2 nanocomposite under the same curing condition. The reasons are probably between the surfaces of nano-SiO_2 with BNPFR molecular exist physical absorption and chemical cross-linking with formation of C-O-Si bond during curing process, which effectively hinder the motion of polymer molecule chains. However, the loss modulus peak temperature T_p for 9 wt% SiO_2 BNPFR/SiO_2 nanocomposite and 12 wt% SiO_2 BNPFR/SiO_2 nanocomposite are not only higher than that of 6wt% SiO_2 BNPFR/SiO_2 nanocomposite, contrary, their T_p are lower than it. Table 1 is the T_p of BNPFR/SiO_2 nanocomposites which has different SiO_2 content. The reasons are probably relative with congregation of nano-SiO_2 when it has a higher content. The result shows that BNPFR and BNPFR/SiO_2 nanocomposite have a highest T_p at 214°C.

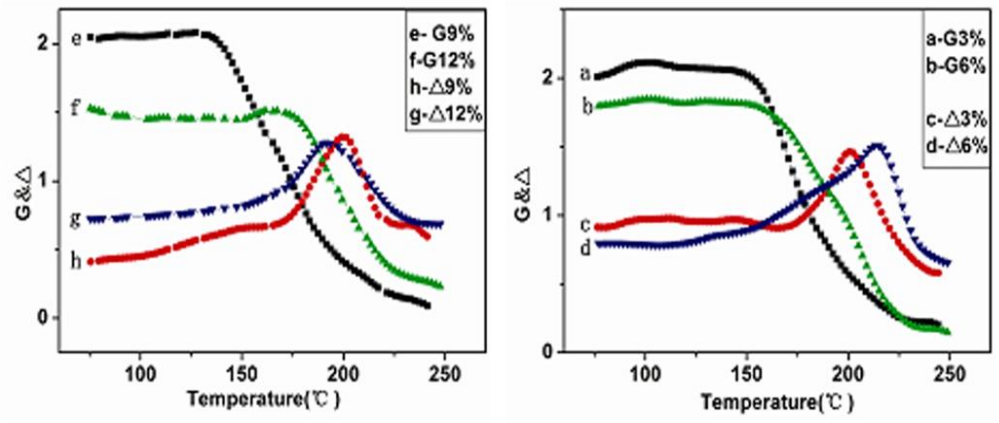

Fig. 4 TBA curves of BNPFR/SiO_2 nanocomposites

Table 1 T_p of BNPFR/SiO_2 naocomposites with different nano-SiO_2 content

	3 %SiO_2	6 % SiO_2	9 % SiO_2	12 % SiO_2
T_p /°C	200	214	199	191

3.4 Thermal stability and degradation Kinetics

In order to investigate the thermal stability of BNPFR and BNPFR/SiO_2 nanocomposites, the resin powders cured 120 min at 180^{o}C were used to determine the thermal weight loss behavior. Fig. 5 shows the TG curves of BNPFR and BNPFR/SiO_2 nanocomposites with different content of nano-SiO_2.

As seen from Fig. 5, the thermal degradation process of BNPFR can be primary divided into two stages. For pure BNPFR, the first degradation stage is from 275 to 350^{o}C, the second degradation stage is from 376 to 800^{o}C. For BNPFR/SiO_2 nanocomposites, the thermal degradation process can be primary divided into three stages. The first degradation stage is from 306 to 466^{o}C, which is higher 25-30^{o}C than BNPFR; the second degradation stage is from 467 to 606^{o}C; the third stage is 607 to 800^{o}C. Table 2 shows the residual weight (%) of resins at different temperature. As seen from Fig. 5 and Tab. 2, the nanocomposite has a higher starting degradation temperature and a higher residual weight than pure BNPFR before 700^o C. The reason is probably that in-situ formed nano-SiO_2 can adsorb a mass of polar groups in BNPFR, and form strong interaction with molecular chain of BNPFR, which include physical absorption and chemical cross-linking with formation of C-O-Si bond. So the thermal stability of BNPFR was improved by the in-situ formed nano-SiO_2. Particular, it has a higher residual weight and increase with increasing SiO_2 content.

To determine the kinetic parameters of thermal decomposition from the thermo-gravimetric data, the first step is to evaluate the conversion of reaction. The weight change of sample is regarded as a function of temperature and the conversion α can be expressed as flows

$$\alpha = \frac{W_0 - W_T}{W_0 - W_\infty} \tag{1}$$

where W_o is the sample weight in *i* stage, W_T is the residual weight of the sample at temperature *T*,

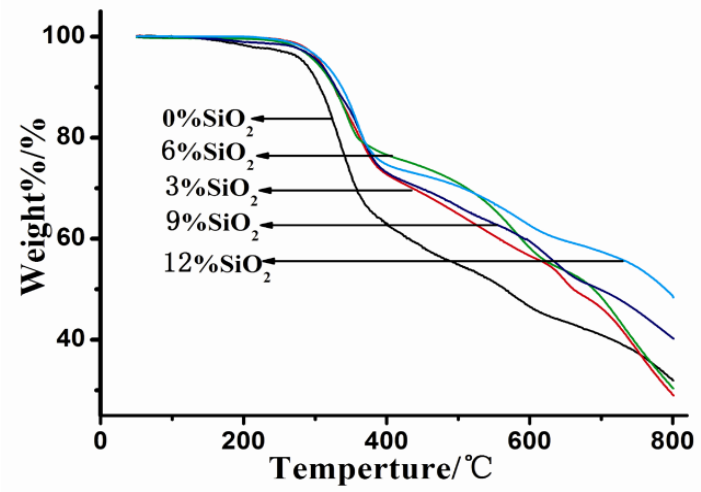

Fig. 5 TG curves of BNPFR/SiO_2 with different nano-SiO_2

Table 2 The residual rate of SiO_2/BNPFR nanocomposites at different temperature

SiO_2/BNCFR	0 %SiO_2	3 %SiO_2	6 %SiO_2	9 %SiO_2	12 %SiO_2
300 ^oC	91.69	96.03	95.07	95.57	96.33
400 ^oC	62.98	72.75	76.64	73.17	74.73
600 ^oC	46.46	56.55	58.13	59.39	62.61
deducting SiO_2	46.46	53.55	52.13	50.39	50.61
700 ^oC	40.91	46.17	48.34	49.76	57.39
deducting SiO_2	40.91	44.51	45.04	44.79	51.58
800 ^oC	31.99	29.16	30.50	40.32	48.76
deducting SiO_2	31.99	25.97	24.36	31.22	36.37

$$\frac{\mathrm{d}\alpha}{\mathrm{d}t} = k(T)\, f(\alpha) \tag{2}$$

$$k(T) = A\exp(-\frac{E_\mathrm{a}}{RT}) \tag{3}$$

W_∞ is the final weight at that stage. Therefore, According TGA curves and Eq. (1), the conversions are calculated for different degradation stages.

In solid-state reaction system, the kinetics of thermal degradation is described as follows

Where $\mathrm{d}\alpha/\mathrm{d}t$ is the degradation rate, Eq. (3) is the Arrhenius equation, A is the pre-exponential factor in the Arrhenius equation, E_a is the apparent activation energy, R is the universal gas constant, T is the absolute temperature. In TGA experiments, heating rate $\beta = \mathrm{d}T/\mathrm{d}t$ is a constant, so heating rate is regarded as a function of temperature, which depends on the time. So the reaction rate can be expressed as

$$\frac{\mathrm{d}\alpha}{\mathrm{d}t} = \frac{\mathrm{d}\alpha}{\mathrm{d}T}\cdot\frac{\mathrm{d}T}{\mathrm{d}t} = \beta\frac{\mathrm{d}\alpha}{\mathrm{d}T} \tag{4}$$

$$\frac{\mathrm{d}\alpha}{\mathrm{d}T} = \frac{A}{\beta}\exp(-\frac{E_\mathrm{a}}{RT})\cdot f(\alpha) \tag{5}$$

By applying the temperature integral term to Eq. (5), we can obtain Eq. (6) as follow

$$G(\alpha) = \int_0^\alpha \frac{\mathrm{d}\alpha}{f(\alpha)} = \frac{A}{\beta}\int_0^\alpha \exp(-\frac{E_\mathrm{a}}{RT})\mathrm{d}T \tag{6}$$

where $G(\alpha)$ is the integral form of the conversion dependence function, the correct form of $G(\alpha)$ depends on the proper reaction mechanism. Differential expression of $G(\alpha)$ for some

Table 3 The kinetic parameters of thermal degradation of 9%SiO_2 BNPFR/SiO_2 Nanocomposite at 20°C/min heating rate

9%SiO_2/BNCFR	*n*	r	E_a /kJ·mol^{-1}	lnA/s^{-1}	a
	1	0.9963	134.02	21.21	0.0664
1st Stage	2	0.9285	64.29	8.31	0.1661
	3	0.9371	138.37	24.14	0.3331
	1	0.9946	99.66	9.36	0.0541
2nd Stage	2	0.9364	63.59	4.84	0.165
	3	0.9382	148.80	19.16	0.3918
	1	0.9925	90.74	5.33	0.0584
3rd Stage	2	0.8973	78.15	4.86	0.2212
	3	0.9301	143.50	14.33	0.3755

solid-state reaction mechanism can be described as following: in first order (n =1), $G(\alpha)$ is –ln (1-α); in second order (n = 2), $G(\alpha)$ is 1/(1 - α); in third order (n = 3), $G(\alpha)$ is 1/(1 - α)^2 (Maron *et al*. 1974).

In this work, because of the degradation of BNPFR/SiO_2 nanocomposite is a mult-stage process, the TGA data were analyzed base on the Madhusdanan-Krishnan-Ninan method (MKN method) (Madhusudanan *et al*.1986), which can be expressed by the following equation

$$\ln(G(\alpha)/T^{1.92}) = \ln\frac{AE_a}{\beta R} + 3.77 - 1.92\ln E_a - \frac{E_a}{RT} \quad (7)$$

where A, R, E_a, β and T had same meanings with the forenamed equations. According to the principle that the probable mechanism has higher linear correlation coefficient value (r) and lower standard deviation value (a), the probable mechanism functions are deduced from the calculated results and shows in Table 3. As seen from Table 3, the two degradation stages are all following first order kinetic mechanism. The activation energy E_a can be obtained from plots of ln [$(G(\alpha)/T^{1.92}$] vs. 1/T and are listed in Table 3.

3.5 Hydrolytic stability

The hydrolytic stability of resins was determined by a half-life of acid-base titration method (Shen *et al*. 1999) and show in Table 4. As seen from Table 4, the BNPFR has a better hydrolytic stability, when the boron content is all 0.00175 mol, the color change time of BPFR is only 1 min, though BNPFR is 36 min, which is 36 times longer than BPFR, for 0.0525 mol amount, the BPFR is 21 min, though BNPFR is 145 min, which is 7 times longer than BPFR. The hydrolysis time is associated with dosage of glycerol added in BNPFR, the more glycerol added, the shorter hydrolysis time. Though, these data have shown that the BNPFR has a better hydrolytic stability than BPFR. This is because the boron atom exhibit three valence, in the BNPFR has a coordination structure of B←N, in here, the shell electronic configuration of the boron atom has a noble gas or octet configuration, so the BNPFR has a better hydrolytic stability than general boron-containing phenol-formaldehyde resin.

4. Conclusions

The boron-nitrogen-containing phenol-formaldehyde resin (BNPFR) can be synthesized from Phenol, boric acid, aminoethyl alcohol and paraformaldehyde. The BNPFR/SiO_2 nanocomposite can be prepared in-situ by ethanolysis of Tetramethoxysilane in BNPFR solution. The nano-SiO_2 with about 50nm diameter has more homogeneous distribution in the samples. The loss modulus peak temperature T_p of BNPFR/SiO_2 nanocomposite is 214^{o}C when nano-SiO_2 content is 6wt%. The start thermal degradation temperature T_{di} is higher about 30^{o}C than pure BNPFR. The residual rate (%) of the nanocomposites at 800 ^{o}C is above 40% when nano-SiO_2 content is 9%.

6. Acknowledgment

The authors appreciate the financial supports from National Nature Science Fund of China The authors gratefully acknowledge the financial support from the Nature Science Foundation (No. E2010000287) of Hebei Province, China.

References

De, D, Adhikari, B. and De, D. (2007), "Grass fiber reinforced phenol formaldehyde resin composite: preparation, characterization and evaluation of properties of composite", *Polym. Advan. Technol*., **18,** 72-81.

Abdalla, O.M, Ludwick, A. and Mitchell, T. (2003), "Boron-modified phenolic resins for high performance applications", *Polymer*, **44**, 7353-7359.

Martin, C., Ronda, J.C. and Cadiz, V. (2006), "Development of novel flame-retardant thermosets based on boron-modified phenol–formaldehyde resins", *J. Polym. Sci. Part A: Polym. Chem*., **44**, 3503-3512.

Liu Y.F., Gao J.G. and Zhang, R.Z. (2002), "Thermal properties and stability of boron-containing phenol-formaldehyde resin formed from paraformaldehyde", *Polym. Degrad. Stabil*., **77**, 495-501.

Gao, J.G. and Xia, L.Y. (2004), "Structure of a boron-containing bisphenal-F formaldehyde resin and kinetics of its thermal degradation", *Polym. Degrad. Stabil*., **83**, 71-77.

Gao, J.G., Jiang, C.J. and Su, X.H. (2010), "Synthesis and thermal properties of boron-nitrogen containing phenol formaldehyde resin/O-MMT Nanocomposite", *Int. J. Polym. Mater*., **59**, 544-552.

Wang, D.C., Chang, G.W. and Chen, Y. (2008), "Preparation and thermal stability of boron- containing phenolic resin/clay nanocomposites", *Polym. Degrad. Stabil*., **93**, 125-133.

Hoofel, H.B., Kiessling, H.J., Lampert, F. and Schonrogge, B. (1975), "Process for the manufacture of curable and thermositting sythesic resins containing nitrogen and boron", *German Patent*, 2436 360 and 2436359**.**

Siramanont, J., Tangpasuthadol, V., Intasiri, A., Ranong, N.N. and Kiatkamjornwong, S. (2009), "Sol-gel process of alkyltriethoxysilane in latex for alkylated silica formation in natural rubber", *Polym. Eng. Sci*., **49**, 1099-1106.

Yuvaraj, H., Shim, J.J. and Lim, K.T. (2010), "Organic-inorganic polypyrrole-surface modified SiO_2 hybrid nanocomposites: a facile and green synthetic approach", *Polym. Advan. Technol*. **21**, 424- 429.

Rund, A.Z. and Eileen, H.J. (2012), "The influence of processing route on the structuring and properties of high-density polyethylene (HDPE)/clay nanocomposites", *Polym. Eng. Sci*., **52,** 2360-2368.

Nayak, T., Khastgir, D. and Chaki, T.K. (2012), "Influence of carbon nanofibers reinforcement on thermal and electrical behavior of polysulfone nanocomposites", *Polym. Eng. Sci*., **52**, 2424-2434.

Kusmono, Z.A., Ishak, M., Chow, W.S., Takeichi, T., Rochmadi, (2010), "Effects of compatibilizers and testing speeds on the mechanical properties of organophilic montmorillonite filled polyamide

6/polypropylene nanocomposites", *Polym. Eng. Sci.* **50**, 1493-1504.
Chiang, C. and Ma, C.M. (2004), "Synthesis, characterization, thermal properties and flame retardance of novel phenolic resin/silica nanocomposites", *Polym. Degrad. Stabil.* **83**, 207-214.
Byun, H.Y., Choi, M.H. and Chung, I.J. (2001), "Synthesis and characterization of resol type phenolic resin/layered silicate nanocomposites", *Chem. Mater.*, **13,** 4111-4226.
Gao, J.G., Jiang, C.J. (2008), "Organic-inorganic hybrid boron-containing phenol-formaldehyder resin/SiO2 nanocomposites", *Polym. Composit.*, **29**, 274-279.
Zhai, D., Gao, J.G., Tian, Q. and Jiang, C.J. (2008), "Thermal degradation kinetics and thermal properties of boron-nitrogen coordination phenol-formaldehyde resin", *Chinese J. Hebei Univ. Nature Sci. Edu.*, **28,** 286-290.
Shen, G., Zheng, Z, Wan, T., Cao, L., Yue, Q. and Sun, T. (1999), "Hydrolytic stability and triboligical properties of organic borate esters as lubricant additives", *Chinese J. Qinghua Univ. Nature Sci. Edu.*, **39**, 97-100.
Shen, D. (1982), *Application of Infrared Spectrum in Polymer*, China Science Press, Beijing, P 88-100.
Tu, W.R. and Wui, S.Y. (1981), "Synthesis boron-containing bisphenol-A formaldehyde resin by formalin method", *Chin. Plast. Indu.*, **4**, 16-18.
Gao, J.G. (1990), "Study on the mechanism of synthesis and curing of boron-containing phenol-formaldehyde resin", *Acta chimica sinica*, **48**, 411- 414.
Gillham, J.K. (1997), The TBA torsion pendulum: a technique for characterizing the cure and properties of thermosetting systems, *Polym. Int.*, **44**, 262-276, 1997.
Brandalise, R.N., Zeni, M., Martins, J.D.N. and Forte, M.M.C. (2009), "Mechanical and dynamic mechanical properties of recycled high density polyethylene and poly (vinyl alcohol) blends", *Polymer. Bulletin.*, **62**, 33-43.
Venditti, R.A. and Gillham, J.K. (1997), "A relationship between the glass transition temperature (T_g) and fractional conversion for thermosetting systems", *J. Appl. Polym. Sci.*, **64**, 3-14.
Doyle, M. Hagstrand, P.O., Manson, J.A.E., Svensson, L. and Lundmark, S. (2003), *Polym. Eng. Sci.*, **43**, 297-305.
Maron, S.H. and Lando, J.B., (1974), *Fundamentals of physical chemistry*, Macmillan Publishing
Co.: New York, 676-687.
Madhusudanan, P.M., Krishnan, K. and Ninan, K.N. (1986), New approximation for the p(x) function in the evaluation of non-isothermal kinetic data, *Thermochim. Acta.*, **97**, 189-201.